Momentum of light scattered from collections of particles

Zhisong Tong and Olga Korotkova

Phys. Rev. A **84**, 043835 — Published 20 October 2011

DOI: 10.1103/PhysRevA.84.043835

Momentum of light scattered from collections of particles

Zhisong Tong and Olga Korotkova

Physics Department, University of Miami, Miami FL 33146

Abstract

The angular dependence of the momentum flow of a polychromatic plane wave scattered from deterministic and random collections of particles is determined, under the conditions of the first Born approximation, as a function of individual and collective properties of particles. The results are of importance for optimization of optical tweezers.

1. Introduction

In applications involving optical trapping of particles, such as optical tweezers which recently gained popularity [1, 2], it is crucial to determine and control the momentum flow of the electromagnetic field. The momentum flow at any spatial position and time instant can be found from the Maxwell stress tensor. The basic theory on this subject relating to monochromatic fields can be found in classic text [3], and its extension to partially coherent fields belongs to Ref. [4] in space-time domain and to Ref. [5] in space-frequency domain, including the corresponding momentum conservation laws.

In optical tweezers it is crucial not only to control the momentum flow of the field incident on the particles but also to predict its behavior upon scattering. The purpose of this work is to evaluate the angular distribution of the momentum flow of an electromagnetic field scattered by a deterministic or random media, which may be a single scatterer or a collection, and to elucidate how the momentum flow of the scattered light wave relates to the individual and collective properties of the scatterers. To illustrate our theoretical analysis, we consider a pair of numerical examples in which a polychromatic electromagnetic plane wave is scattered from a collection of identical particles having deterministic potentials and either deterministic or random locations.

2. Momentum flow of an electromagnetic field on weak scattering

We begin by considering a polychromatic electromagnetic vector-field $\mathbf{E}^{(i)}(\mathbf{r},\omega)=\left[E_x^{(i)}(\mathbf{r},\omega),E_y^{(i)}(\mathbf{r},\omega),E_z^{(i)}(\mathbf{r},\omega)\right]$ at a point with position-vector $\mathbf{r}$, at angular frequency ω, which is incident onto a medium with volume V where only the polarization, $\mathbf{P}(\mathbf{r},\omega)$, is induced, i.e. only the electric properties of the medium modulate the field in a

nontrivial fashion. It is the case for most substances. Specialized to polychromatic fields, the scattered electric and magnetic fields outside the scattering volume V may be expressed, respectively, as (Ref. [6], Sec. 13.6)

$$\mathbf{E}^{(s)}(\mathbf{r},\omega) = \nabla\times\nabla\times\mathbf{\Pi}_e(\mathbf{r},\omega), \tag{1}$$

$$\mathbf{B}^{(s)}(\mathbf{r},\omega) = -ik\nabla\times\mathbf{\Pi}_e(\mathbf{r},\omega), \tag{2}$$

where $\mathbf{\Pi}_e$ is the electric Hertz potential defined by

$$\mathbf{\Pi}_e(\mathbf{r},\omega) = \int_V \mathbf{P}(\mathbf{r}',\omega)G(\mathbf{r}-\mathbf{r}')d^3r', \tag{3}$$

where $\mathbf{r}'$ is a point within volume V and

$$G(\mathbf{R}) = G(R) = \frac{\mathrm{e}^{ikR}}{R}, \tag{4}$$

is the free-space Green's function for the Helmholtz equation. Further, if the response of the medium is linear and the scattering is sufficiently weak, the constitutive relation may be expressed, within the accuracy of the first-order Born approximation, as [7]

$$\begin{aligned}\mathbf{P}(\mathbf{r}',\omega) &= \eta(\mathbf{r}',\omega)\mathbf{E}^{(i)}(\mathbf{r}',\omega)\\ &= \frac{1}{k^2}F(\mathbf{r}',\omega)\mathbf{E}^{(i)}(\mathbf{r}',\omega),\end{aligned}, \tag{5}$$

where η is the dielectric susceptibility and F is the scattering potential of the medium defined by expression

$$F(\mathbf{r}',\omega) = \begin{cases}\dfrac{1}{4\pi}k^2[n^2(\mathbf{r}',\omega)-1] & \mathbf{r}'\in V,\\ 0 & \mathbf{r}'\notin V.\end{cases} \tag{6}$$

It is often of interest in scattering experiments to examine the behavior of the scattered field in the far zone. By denoting $\mathbf{r} = r\mathbf{s}$, $\mathbf{s}$ being the unit vector along direction $\mathbf{r}$ (see Fig. 1), we can approximate the free-space Green's function by the form

$$\frac{\mathrm{e}^{ik|\mathbf{r}-\mathbf{r}'|}}{|\mathbf{r}-\mathbf{r}'|} = \frac{\mathrm{e}^{ikr}}{r}\mathrm{e}^{-ik\mathbf{s}\cdot r'}. \tag{7}$$

On substituting from Eqs. (3), (5) and (7) into Eq. (1) we find that the scattered electric field in the far zone becomes ([8], see also [9])

$$\mathbf{E}^{(s)}(\mathbf{r},\omega)=\frac{\mathrm{e}^{ikr}}{r}\int_V F(\mathbf{r}',\omega)\mathbf{E}^{(i)}(\mathbf{r}',\omega)\circ\hat{\mathbf{S}}_1(\mathbf{s})\,\mathrm{e}^{-ik\mathbf{s}\cdot r'}\,d^3r', \tag{8}$$

where circle stands for matrix multiplication (not to be confused with dot product and cross-product) and tensor $\hat{\mathbf{S}}_1(\mathbf{s})$ in the explicit form is

$$\hat{\mathbf{S}}_1(\mathbf{s})=\begin{pmatrix}1-s_x^2 & -s_xs_y & -s_xs_z\\ -s_ys_x & 1-s_y^2 & -s_ys_z\\ -s_zs_x & -s_zs_y & 1-s_z^2\end{pmatrix}. \tag{9}$$

Similar procedure leads to the expression of the scattered magnetic field in the far zone:

$$\mathbf{B}^{(s)}(\mathbf{r},\omega)=\frac{\mathrm{e}^{ikr}}{r}\int_V F(\mathbf{r}',\omega)\mathbf{E}^{(i)}(\mathbf{r}',\omega)\circ\hat{\mathbf{S}}_2(\mathbf{s})\,\mathrm{e}^{-ik\mathbf{s}\cdot r'}\,d^3r', \tag{10}$$

with

$$\hat{\mathbf{S}}_2(\mathbf{s})=\begin{pmatrix}0 & s_z & -s_y\\ -s_z & 0 & s_x\\ s_y & -s_x & 0\end{pmatrix}. \tag{11}$$

We note that equations (8) and (10) are the same transformation laws in form, except they involve different transformation matrices, (9) and (11), respectively. In particular, $\hat{\mathbf{S}}_1$ is a symmetric matrix while $\hat{\mathbf{S}}_2$ is anti-symmetric. Further, since $\mathbf{s}\cdot\mathbf{E}^{(s)}=0$, $\mathbf{s}\cdot\mathbf{B}^{(s)}=0$, and $\mathbf{B}^{(s)}=\mathbf{s}\times\mathbf{E}^{(s)}$, the scattered electromagnetic field is the outgoing spherical wave which propagates in the direction of the unit vector $\mathbf{s}$, i.e. in the outward radial direction from the scatterer. The incident field and the transformation matrices are all expressed in the Cartesian coordinate system, hence the resulting scattered fields are also in the same system. Then the total field including the incident filed and the scattered field may be expressed

$$\mathbf{E}(\mathbf{r},\omega)=\mathbf{E}^{(i)}(\mathbf{r},\omega)+\mathbf{E}^{(s)}(\mathbf{r},\omega), \tag{12a}$$

$$\mathbf{B}(\mathbf{r},\omega)=\mathbf{B}^{(i)}(\mathbf{r},\omega)+\mathbf{B}^{(s)}(\mathbf{r},\omega). \tag{12b}$$

The fields considered are out of the dielectric materials to avoid the Abraham-Minkowski controversy [10]. The Maxwell stress tensor $\mathbf{T}(\mathbf{r},\omega)$ of a monochromatic field in the space-frequency domain was shown to be given by the formula [5]

$$\mathbf{T}(\mathbf{r},\omega)=\frac{1}{4\pi}\left\{\mathbf{E}^{\dagger}(\mathbf{r},\omega)\circ\mathbf{E}(\mathbf{r},\omega)-\frac{1}{2}Tr\left[\mathbf{E}^{\dagger}(\mathbf{r},\omega)\circ\mathbf{E}(\mathbf{r},\omega)\right]\hat{\mathbf{I}}\right\}$$

$$+\frac{1}{4\pi}\left\{\mathbf{B}^{\dagger}(\mathbf{r},\omega)\circ\mathbf{B}(\mathbf{r},\omega)-\frac{1}{2}Tr\left[\mathbf{B}^{\dagger}(\mathbf{r},\omega)\circ\mathbf{B}(\mathbf{r},\omega)\right]\hat{\mathbf{I}}\right\}, \tag{13}$$

where $\hat{\mathbf{I}}$ is a unit 3×3 matrix and Tr stands for the trace of a matrix. Then the momentum flow $\mathbf{Q}(r\mathbf{s})$ is defined, as a function of normal direction $\mathbf{s}$, as

$$\mathbf{Q}(r\mathbf{s})=\mathbf{s}\cdot\mathbf{T}(\mathbf{r},\omega)\,. \tag{14}$$

The total change in momentum within the volume V containing the scattering media can be identified as the sum of the change in mechanical momentum of the scattering media and the change in the momentum of enclosed electromagnetic fields. According to the momentum conservation law the total change in momentum is equal to the net momentum flow introduced by the total field, through the surface enclosing volume V, which may be predicted by Eq. (14).

3. Momentum flow of a scattered polychromatic plane wave.

Let us now confine our analysis to the case of an incident polychromatic plane wave propagating along the $z-$axis, i.e. having wave vector $\mathbf{s}_0=[0,0,1]$ (see Fig. 1):

$$E_j^{(i)}(\mathbf{r}',\omega)=a_j(\omega)\,\mathrm{e}^{ik\mathbf{s}_0\cdot\mathbf{r}'}\qquad (j=x,y)\,, \tag{15}$$

where $a_j(\omega)$ is the amplitude of the electric field and only the two transverse components, $x-$ and y, are nontrivial. The magnetic counterpart of the incident field, $\mathbf{B}^{(i)}(\mathbf{r}',\omega)=\mathbf{s}_0\times\mathbf{E}^{(i)}(\mathbf{r}',\omega)$, (Ref. [6], Sec. 1.4) may be expressed, for the planar wave-front, as

$$\mathbf{B}^{(i)}(\mathbf{r}',\omega)=\mathbf{E}^{(i)}(\mathbf{r}',\omega)\circ\hat{\mathbf{S}}_2(\mathbf{s}_0)\,, \tag{16}$$

where $\mathbf{B}^{(i)}(\mathbf{r}',\omega)=\left[B_x^{(i)}(\mathbf{r}',\omega),B_y^{(i)}(\mathbf{r}',\omega),B_z^{(i)}(\mathbf{r}',\omega)\right]$ and

$$\hat{\mathbf{S}}_2(\mathbf{s}_0)=\begin{pmatrix}0&1&0\\-1&0&0\\0&0&0\end{pmatrix}. \tag{17}$$

where the $\hat{\mathbf{S}}_2$ matrix is introduced in Eq. (11). In a general case when either the incident field is stochastic, wide-sense statistically stationary and/or scattering medium acts on the incident field in a random but static manner the resulting scattered electromagnetic field is also wide-sense statistically stationary [11]. To characterize the second-order correlation properties of

fluctuating fields we use the cross-spectral density tensors at coinciding spatial arguments for its electric and magnetic counterparts as follows [11]

$$\mathbf{W}^{E}(\mathbf{r},\mathbf{r},\omega)=\left\langle \mathbf{E}^{\dagger}(\mathbf{r},\omega)\circ\mathbf{E}(\mathbf{r},\omega)\right\rangle, \tag{18}$$

$$\mathbf{W}^{B}(\mathbf{r},\mathbf{r},\omega)=\left\langle \mathbf{B}^{\dagger}(\mathbf{r},\omega)\circ\mathbf{B}(\mathbf{r},\omega)\right\rangle, \tag{19}$$

dagger standing for Hermitian adjoint, and angular brackets denoting the ensemble average in the sense of classic coherence theory in the space-frequency domain.

On substituting from Eq. (15) into Eq. (18) we find that at coinciding spatial arguments the electric cross-spectral density matrix of the incident polychromatic plane wave has the form

$$\mathbf{W}^{(ii),E}(\mathbf{r},\mathbf{r},\omega)=S^{(i)}(\omega)\mathbf{C}, \tag{20}$$

where $\left\langle a_i^{*}(\omega)a_j(\omega)\right\rangle = A_iA_jB_{ij}S^{(i)}(\omega)$, star standing for complex conjugate, and tensor

$$\mathbf{C}=\begin{pmatrix} A_x^2 & A_xA_yB & 0\\ A_yA_xB & A_y^2 & 0\\ 0 & 0 & 0\end{pmatrix} \tag{21}$$

characterizes the correlation properties between the mutually orthogonal components of the field. In a similar way we find that the correlation tensor of the incident magnetic fields has the form

$$\mathbf{W}^{(ii),B}(\mathbf{r},\mathbf{r},\omega)=-S^{(i)}(\omega)\hat{\mathbf{S}}_2(\mathbf{s}_0)\circ\mathbf{C}\circ\hat{\mathbf{S}}_2(\mathbf{s}_0), \tag{22}$$

where the negative sign results from the anti-symmetry of tensor $\hat{\mathbf{S}}_2(\mathbf{s}_0)$.

The correlation tensors of the scattered electric and magnetic fields can also be determined on substituting from Eq. (8) into Eq. (18) and from Eq. (10) into Eq. (19), using Eq. (20) respectively:

$$\mathbf{W}^{(ss),E}(\mathbf{r},\mathbf{r},\omega)=\frac{1}{r^2}C_F(-\mathbf{K},\mathbf{K},\omega)\hat{\mathbf{S}}_1(\mathbf{s})\circ\mathbf{W}^{(ii),E}(\mathbf{r},\mathbf{r},\omega)\circ\hat{\mathbf{S}}_1(\mathbf{s})$$

$$=\frac{1}{r^2}S^{(i)}(\omega)C_F(-\mathbf{K},\mathbf{K},\omega)\hat{\mathbf{S}}_1(\mathbf{s})\circ\mathbf{C}\circ\hat{\mathbf{S}}_1(\mathbf{s}), \tag{23}$$

$$\mathbf{W}^{(ss),B}(\mathbf{r},\mathbf{r},\omega)=-\frac{1}{r^2}C_F(-\mathbf{K},\mathbf{K},\omega)\hat{\mathbf{S}}_2(\mathbf{s})\circ\mathbf{W}^{(ii),E}(\mathbf{r},\mathbf{r},\omega)\circ\hat{\mathbf{S}}_2(\mathbf{s})$$

$$= -\frac{1}{r^2} S^{(i)}(\omega) C_F(-\mathbf{K}, \mathbf{K}, \omega) \hat{\mathbf{S}}_2(\mathbf{s}) \circ \mathbf{C} \circ \hat{\mathbf{S}}_2(\mathbf{s}), \tag{24}$$

where $\mathbf{K} = k(\mathbf{s} - \mathbf{s}_0)$ resembles the momentum transfer vector in quantum mechanics and

$$C_F(-\mathbf{K}, \mathbf{K}, \omega) = \int_V \int_V \left\langle F^*(\mathbf{r}_1', \omega) F(\mathbf{r}_2', \omega) \right\rangle_m \mathrm{e}^{-i\mathbf{K}\cdot(\mathbf{r}_2' - \mathbf{r}_1')} \, d^3 r_1' \, d^3 r_2', \tag{25}$$

is the six-dimensional Fourier transform of the correlation function of the scattering potential of the medium, averaged over the ensemble of its realizations which is accounted by angular brackets with subscript *m*.

The total electric field produced on scattering is the sum of the incident electric field and the scattered electric field and, hence, the cross-spectral density tensor of the total field includes a cross-term appearing from their interference. The same is true for the magnetic fields. Thus we have by substituting Eqs. (12a) and (12b) into Eqs. (18) and (19), respectively,

$$\mathbf{W}^E(\mathbf{r}, \mathbf{r}, \omega) = \mathbf{W}^{(ii),E}(\mathbf{r}, \mathbf{r}, \omega) + \mathbf{W}^{(ss),E}(\mathbf{r}, \mathbf{r}, \omega) + \mathbf{W}^{(is),E}(\mathbf{r}, \mathbf{r}, \omega), \tag{26}$$

$$\mathbf{W}^B(\mathbf{r}, \mathbf{r}, \omega) = \mathbf{W}^{(ii),B}(\mathbf{r}, \mathbf{r}, \omega) + \mathbf{W}^{(ss),B}(\mathbf{r}, \mathbf{r}, \omega) + \mathbf{W}^{(is),B}(\mathbf{r}, \mathbf{r}, \omega). \tag{27}$$

where the mixed terms are given by the formulas

$$\mathbf{W}^{(is),E}(\mathbf{r}, \mathbf{r}, \omega) = \left\langle \mathbf{E}^{(s)+}(\mathbf{r}, \omega) \circ \mathbf{E}^{(i)}(\mathbf{r}, \omega) + \mathbf{E}^{(i)+}(\mathbf{r}, \omega) \circ \mathbf{E}^{(s)}(\mathbf{r}, \omega) \right\rangle,$$

$$\mathbf{W}^{(is),B}(\mathbf{r}, \mathbf{r}, \omega) = \left\langle \mathbf{B}^{(s)+}(\mathbf{r}, \omega) \circ \mathbf{B}^{(i)}(\mathbf{r}, \omega) + \mathbf{B}^{(i)+}(\mathbf{r}, \omega) \circ \mathbf{B}^{(s)}(\mathbf{r}, \omega) \right\rangle.$$

We will now turn our attention to calculation of the momentum flow of the scattered field. For electromagnetic stochastic fields the ensemble averaged version of the stress tensor can then be generalized from Eq. (14) as [5]

$$\left\langle \mathbf{T}(\mathbf{r}, \omega) \right\rangle = \frac{1}{4\pi} \left\{ \mathbf{W}^E(\mathbf{r}, \mathbf{r}, \omega) - \frac{1}{2} Tr\left[\mathbf{W}^E(\mathbf{r}, \mathbf{r}, \omega) \right] \hat{\mathbf{I}} \right\}$$

$$+ \frac{1}{4\pi} \left\{ \mathbf{W}^B(\mathbf{r}, \mathbf{r}, \omega) - \frac{1}{2} Tr\left[\mathbf{W}^B(\mathbf{r}, \mathbf{r}, \omega) \right] \hat{\mathbf{I}} \right\}. \tag{28}$$

On substituting from Eqs. (26) and (27) into Eq. (28) we find that in the situation involving scattering the total stress tensor has the following general form:

$$\left\langle \mathbf{T}(\mathbf{r}, \omega) \right\rangle = \left\langle \mathbf{T}^{(i)}(\mathbf{r}, \omega) \right\rangle + \left\langle \mathbf{T}^{(s)}(\mathbf{r}, \omega) \right\rangle + \left\langle \mathbf{T}^{(is)}(\mathbf{r}, \omega) \right\rangle. \tag{29}$$

Here the Maxwell stress tensors of the incident and scattered fields as well as of the mixed term are, respectively:

$$\left\langle \mathbf{T}^{(i)} \right\rangle = \frac{1}{4\pi}\left\{ \left(\mathbf{W}^{(ii),E} + \mathbf{W}^{(ii),B} \right) - \frac{1}{2} Tr\left(\mathbf{W}^{(ii),E} + \mathbf{W}^{(ii),B} \right)\hat{\mathbf{I}} \right\}, \tag{30}$$

$$\left\langle \mathbf{T}^{(s)} \right\rangle = \frac{1}{4\pi}\left\{ \left(\mathbf{W}^{(ss),E} + \mathbf{W}^{(ss),B} \right) - \frac{1}{2} Tr\left(\mathbf{W}^{(ss),E} + \mathbf{W}^{(ss),B} \right)\hat{\mathbf{I}} \right\}, \tag{31}$$

$$\left\langle \mathbf{T}^{(is)} \right\rangle = \frac{1}{4\pi}\left\{ \left(\mathbf{W}^{(is),E} + \mathbf{W}^{(is),B} \right) - \frac{1}{2} Tr\left(\mathbf{W}^{(is),E} + \mathbf{W}^{(is),B} \right)\hat{\mathbf{I}} \right\}, \tag{32}$$

where the arguments of the tensors are suppressed for brevity. In the present work we assume that the interference between the incident and the scattered fields is weak and can be neglected, i.e. $\left\langle \mathbf{T}^{(is)} \right\rangle \approx 0$, which is usually the case. We make such an assumption since a random scattering medium may change the incident field, making the statistical properties of the scattered field completely uncorrelated with the original incident field. Therefore in a majority of recently published papers about scattering, the researchers only consider the correlation properties between the scattered fields themselves (see, for example, Ref.[7], Chap.6; Ref.[8]; Ref. [9]). Then the explicit expression for $\left\langle \mathbf{T}^{(i)} \right\rangle$ may be obtained by substituting from Eqs. (20) and (22) into Eq. (30) as

$$\left\langle \mathbf{T}^{(i)}(\mathbf{r},\omega) \right\rangle = -\frac{1}{4\pi} S^{(i)}(\omega) \begin{pmatrix} 0 & 0 & 0 \\ 0 & 0 & 0 \\ 0 & 0 & A_x^2 + A_y^2 \end{pmatrix}. \tag{33}$$

We note that for the momentum flow of the incident plane wave propagating into a plane perpendicular to radial unit vector $\mathbf{s}$, only the $z-$component is nontrivial since [see Eq. (14)]

$$\mathbf{Q}^{(i)}(r\mathbf{s}) = \mathbf{s} \cdot \left\langle \mathbf{T}^{(i)}(\mathbf{r},\omega) \right\rangle = -\frac{1}{4\pi} S^{(i)}(\omega) \left(0 \quad 0 \quad \left(A_x^2 + A_y^2 \right) s_z \right). \tag{34}$$

On the other hand, for the scattered field the Maxwell stress tensor is a function of radial direction $\mathbf{s}$, which can be readily asserted on substituting from Eqs. (23) and (24) into Eq. (31) , to obtain the expression for the momentum flow $\mathbf{Q}^{(s)}(\mathbf{s})$ of the scattered field as:

$$\mathbf{Q}^{(s)}(r\mathbf{s}) \equiv \mathbf{s} \cdot \left\langle \mathbf{T}^{(s)}(\mathbf{r},\omega) \right\rangle = -\frac{1}{4\pi r^2} S^{(i)}(\omega) C_F(-\mathbf{K},\mathbf{K},\omega) \left(Tr\mathbf{C} - \mathbf{s} \circ \mathbf{C} \circ \mathbf{s}^T \right)\mathbf{s}, \tag{35}$$

where $\mathbf{s} = \left(s_x, s_y, s_z \right)$. Equation (35) is the main result of the paper. It can be used to determine the angular distribution of the momentum flow of the scattered field in the far zone

as it propagates into a plane perpendicular to radial unit vector $\mathbf{s}$. We note that only the field component along the radial direction is nontrivial and is independent of the incident direction. Equation (35) implies that the momentum flow $\mathbf{Q}^{(s)}(r\mathbf{s})$ of the scattered field depends on the correlation function of the potential of the scattering medium and on the correlation properties of the incident field. Thus, there is no net momentum flow for an incident electromagnetic plane wave, even though the angular distribution of the stress tensor is nontrivial. However, as for the momentum flow introduced by the scattered field, its angular distribution does not only depend on the degree of polarization of the incident plane waves, but also upon the distribution of the scattering materials and the correlation properties of the media. Therefore, the net scattered momentum flow is nontrivial, being influenced by physical and statistical properties of the scattering medium.

4. Numerical examples

We will now employ the theoretical development of Sections 2 and 3 for solving an important class of problems relating to angular momentum distribution of light scattered from deterministic and random particulate media. For simplicity we will confine ourselves only to collections of identical particles. The scattering potential of the collection can be expressed as sum

$$F(\mathbf{r}',\omega)=\sum_{m=1}^{N} f(\mathbf{r}'-\mathbf{r}_m,\omega)\,, \tag{36}$$

where $\mathbf{r}_m$ is the center of a particle m. Further, the Fourier transform of the correlation function of the medium then takes form [7]

$$C_F(-\mathbf{K},\mathbf{K},\omega)=\left|f(\mathbf{K},\omega)\right|^2 M(\mathbf{K},\omega)\,, \tag{37}$$

where $f(\mathbf{K},\omega)$ is the Fourier transform of scattering potential of a single particle $f(\mathbf{r}',\omega)$, and $M(\mathbf{K},\omega)=\left\langle\left|\sum_{m=1}^{N}\mathrm{e}^{-i\mathbf{K}\cdot\mathbf{r}_m}\right|^2\right\rangle$ is the structure factor containing the correlation information of the entire particle system. We assume the scattering potential of the particle is of Gaussian distribution, i.e. $f(\mathbf{r}',\omega)=\exp\left[-\frac{\mathbf{r}'^2}{2\sigma^2}\right]$. With $s_x=\sin\theta\cos\varphi$, $s_y=\sin\theta\sin\varphi$ and $s_z=\cos\theta$ (see Fig. 1), we calculate the distribution of the momentum flow of the scattered fields at the scattering plane $\varphi=0$. The parameters of the incident plane wave are chosen to be: $\lambda=0.6328\mu m$, $A_x=A_y=1$, $B=0.2$.

In Fig. 2 we consider the models of particle collections distributed along the x-axis that we use for numerical calculations. In particular, in Fig. 2(a) we show the simplest case of a pair of symmetrically located particles, with centers at $(d/2,0,0)$ and $(-d/2,0,0)$, respectively (Fig. 2(a)). In Figs. 3 and 4 we present the momentum flow of the field scattered from collection of Fig. 2(a). It becomes clear from these two figures that the separation between the two particles influences the number and position of the peaks of the momentum flow, while the size of the particles changes the peak value and retains the position of each peak. To understand the peak positions which are determined by the interference between particles, we first derive, from Eq. (35), the condition for the valley points (i.e., where $\left|Q^{(s)}(s)\right|=0$):

$$d_{sp}\sin\theta=(n+\frac{1}{2})\lambda\,,\quad (n=0,1,2...)\,. \tag{38}$$

where d_{sp} is the spacing distance between two particles. This equation matches the positions of valley points in Figs. 3 and 4 accurately. Therefore for the case where the peak points are about the center of the two neighboring valley points (for example, $kd=8\pi$ and $kd=16\pi$), the peak points' positions may be approximately estimated by the equation

$$d_{sp}\sin\theta=n\lambda\,,\quad (n=0,1,2...)\,. \tag{39}$$

The reason that Eq. (38) is accurate for valley points while Eq. (39) is only approximately correct for the peak points may be explained as follows. In our case we consider the correlation between two scattered fields and, more importantly, we calculate the momentum flow (not just the spectral density). So the quantity [Eq. (35) with Eq. (37)] is not only affected by the interference between the two waves as included in $M(\mathbf{K},\omega)$, but also the properties of the scattering medium, included in $\left|f(\mathbf{K},\omega)\right|^2$, and the properties of the incident field, included in $\left(Tr\mathbf{C}-\mathbf{s}\circ\mathbf{C}\circ\mathbf{s}^T\right)$. The peak points for the interference pattern are moved due to this reason, while the valley points where the spectral density is zero are unchanged since they retain the value zero despite of the product of other terms.

For particles distributed according to Figs. 2(b) - 2(e), the scattered angular distribution of momentum flow is given in Fig. 5. It is interesting to note that there is one maximum peak value around 14° indepenent of the number of particles symmetrically distributed along the x-axis, with the second peak appearing around 30°. This case with more than two particles is a more interesting problem since the interference of the scattered wave would not only come from the two adjacent particles but also from other particles. In our case the interference from multiple particles may be suitably divided into separate interference between two particles. Then for the set-ups in Fig.2, the possible spacing distance between any two particles would be $d/2$, d, $3d/2$, $2d$, $5d/2$, $3d$, $7d/2$, $4d$, $9d/2$, $5d$. For spacing values $d_{sp}=\frac{l}{2}d$ ($l=1,2,...10$) in Eq. (39), the possible peak positions would be (with $kd=16\pi$)

$$\sin\theta=\frac{n}{4l}\,,\ (n=0,1,2...)\,. \tag{40}$$

Therefore for all the possible spacing choices, they share the common the peak position at $\sin\theta_{mm} = 1/4$ with $\theta_{mm} = 14.4775$ degree (mm means major maximum), which explains the first major maximum. For other major maximum, similar explanation applies. And the governing equation for the nth major maximum is $(d/2)\sin\theta = n\lambda$.

From Fig. 5, the fact that the number of minor peaks is equal to half of the number of particles can also be explained by the interference between waves scattered from the particles. It can be assumed the minor peaks are associated with different orders of maxima between two particles with distance equal to $(M+1)d/2$. The reason for this assumption may be explained as follows. Let us consider the most complicated case in Fig. 2e, where $M = 5$. We may obtain the all the possible spacing distances between any two particles and count the numbers that the spacing distance appears. One may see from Table 1 that the peak positions for the spacing distances $d/2$, d, $3d/2$ are overlapped by the peak positions for the spacing $3d$. And the counting number for spacing $3d$ is greater than other spacing possibilities except $d/2$, d and $3d/2$, whose peak positions have been overlapped. Therefore the minor peak positions may be dominated by the different orders of maximum of distance $3d$, although the exact minor peak positions may be slightly different due to the existence of interference of other choices of spacing distances. Furthermore, $3d = (M+1)d/2$, where $M = 5$ is the number of particles at one side of origin. Other cases with different number of particles may be similarly analyzed.

In Fig. 6 we consider a special case of a gas-like disorder [12] where identical particles with Gaussian potentials randomly positioned along the x-axis. In this case the particles are considered as statistically independent. Then structure factor becomes $M(\mathbf{K},\omega) = N = \frac{1}{N}M(0,\omega)$ for all $\mathbf{K}$ except $\mathbf{K} = 0$. Figure 6 shows the angular distribution of momentum flow of the scattered far field from $N = 5$ and $N = 10$ particles, respectively. The range of x-axis within which all the particles are randomly distributed is 40λ, i.e., -20λ 20λ. Therefore, the average spacing between neighboring particles for 10 particles is 4λ and for 5 particles is 8λ, respectively. In each case the momentum flow is the statistical average over 30 realizations. The the absolute value of momentum flow $\left|\mathbf{Q}^{(s)}(r\mathbf{s})\right|$ decreases abruptly to a value on the order of 1/N over the several degrees from the forward scattering direction and then levels off with a small negative slope due to the additional terms in Eq. (35). The fluctuations in the tail of $\left|\mathbf{Q}^{(s)}(r\mathbf{s})\right|$ are caused by the limited number of particles in the ensemble: for sufficiently large values of N the momentum flow drops to zero over the first several degrees.

In summary, we have derived the expression for the angular distribution of the momentum flow of the field produced on scattering of a plane wave from random media, which can be a single particle or collection as well as of deterministic or random nature. We have found that both polarization properties of the incident electromagnetic plane wave and the scattering potentials of the scattering material influence the distribution of the momentum flow of the scattered field. From the examples considered, the size of particles, the separation between

them, and the nature of the collection (deterministic or random centers' locations) significantly influence the angular distribution of the momentum flow throughout the far zone of the scatterer.

Acknowledgments

This work is supported by AFOSR 95500810102 and ONR N0016111RCZ0604.

References

1. A. Ashkin, J. M. Sdiedzic, J. E. Bjorkholm and S. Chu, Opt. Lett. **11**, 288 (1986).
2. K. C. Neuman and S. M. Block, Rev. Sci. Instr. **75**, 2787 (2004).
3. J. D. Jackson, *Classical Electrodynamics*, 2nd ed. (Wiley, New York, 1975).
4. P. Roman and E. Wolf, Nuovo Cimento 17, 477 (1960).
5. S. M. Kim and G. Gbur, Phy. Rev. A **79**, 033844 (2009).
6. M. Born and E. Wolf, *Principles of Optics* (Cambridge University Press, Cambridge, 1999).
7. E. Wolf, *Introduction to the Theory of Coherence and Polarization of Light* (Cambridge U. Press, 2007).
8. Z. Tong and O. Korotkova, Phys. Rev. A **82**, 033836 (2010).
9. T. Wang and D. Zhao, Opt. Lett. **35**, 2412 (2010).
10. R. N. C. Pfeifer, T. A. Nieminen, N. R. Heckenberg and H. Rubinsztein-Dunlop, Rev. Mod. Phys. **79**, 1197 (2007).
11. L. Mandel and E. Wolf, *Optical Coherence and Quantum Optics* (Cambridge University Press, Cambridge, 1995).
12. J. M. Ziman, *Models of Disorder* (Cambridge U. Press, 1979).

Complete List of References

1. A. Ashkin, J. M. Sdiedzic, J. E. Bjorkholm and S. Chu, "Observation of a single-beam gradient force optical trap for dielectric particles", Opt. Lett. **11**, 288 (1986).
2. K. C. Neuman and S. M. Block, "Optical Trapping", Rev. Sci. Instr. **75**, 2787 (2004).
3. J. D. Jackson, *Classical Electrodynamics*, 2nd ed. (Wiley, New York, 1975).
4. P. Roman and E. Wolf, "Correlation theory of stationary electromagnetic fields—part II: conservation laws", Nuovo Cimento 17, 477 (1960).
5. S. M. Kim and G. Gbur, "Momentum conservation in partially coherent wave fields", Phy. Rev. A **79**, 033844 (2009).
6. M. Born and E. Wolf, *Principles of Optics* (Cambridge University Press, Cambridge, 1999).
7. E. Wolf, *Introduction to the Theory of Coherence and Polarization of Light* (Cambridge U. Press, 2007).
8. Z. Tong and O. Korotkova, "Theory of weak scattering of stochastic electromagnetic fields from deterministic and random media", Phys. Rev. A **82**, 033836 (2010).
9. T. Wang and D. Zhao, "Scattering theory of stochastic electromagnetic light waves", Opt. Lett. **35**, 2412 (2010).
10. R. N. C. Pfeifer, T. A. Nieminen, N. R. Heckenberg and H. Rubinsztein-Dunlop, "Colloquium: Momentum of an electromagnetic wave in dielectric media", Rev. Mod. Phys. **79**, 1197 (2007).
11. L. Mandel and E. Wolf, *Optical Coherence and Quantum Optics* (Cambridge University Press, Cambridge, 1995).
12. J. M. Ziman, *Models of Disorder* (Cambridge U. Press, 1979).

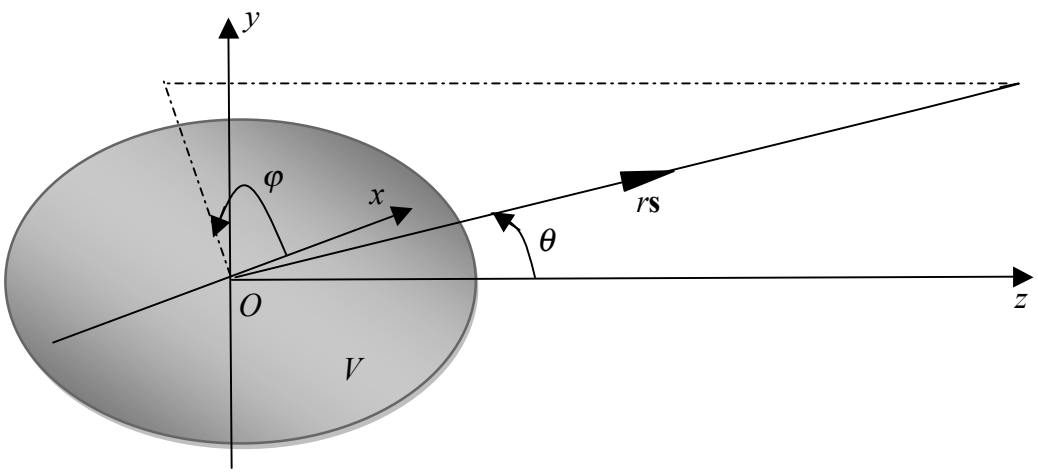

Fig. 1 Illustration of notations of spherical coordinate system.

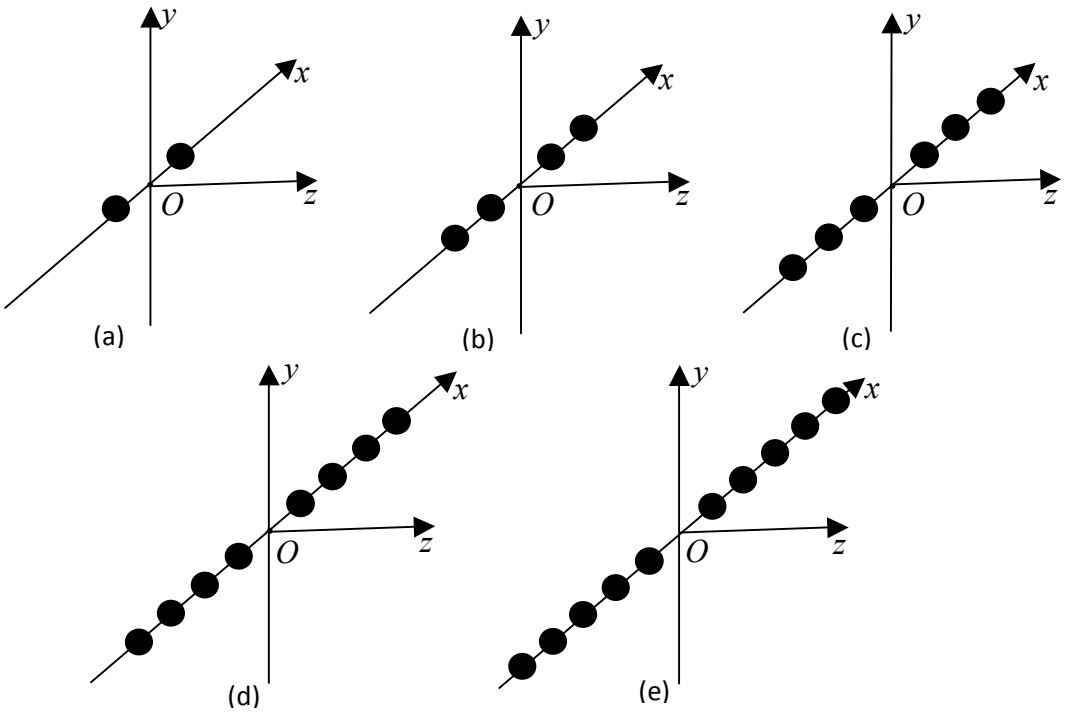

Fig. 2 The coordinates of particles (a) (d/2,0,0), (-d/2,0,0); (b) (d/2,0,0), (-d/2,0,0), (d,0,0), (-d,0,0); (c) (d/2,0,0), (-d/2,0,0), (d,0,0), (-d,0,0), (3d/2,0,0), (-3d/2,0,0); (d) (d/2,0,0), (-d/2,0,0), (d,0,0), (-d,0,0), (3d/2,0,0), (-3d/2,0,0), (2d,0,0), (-2d,0,0); (e) (d/2,0,0), (-d/2,0,0), (d,0,0), (-d,0,0), (3d/2,0,0), (-3d/2,0,0), (2d,0,0), (-2d,0,0), (5d/2,0,0), (-5d/2,0,0).

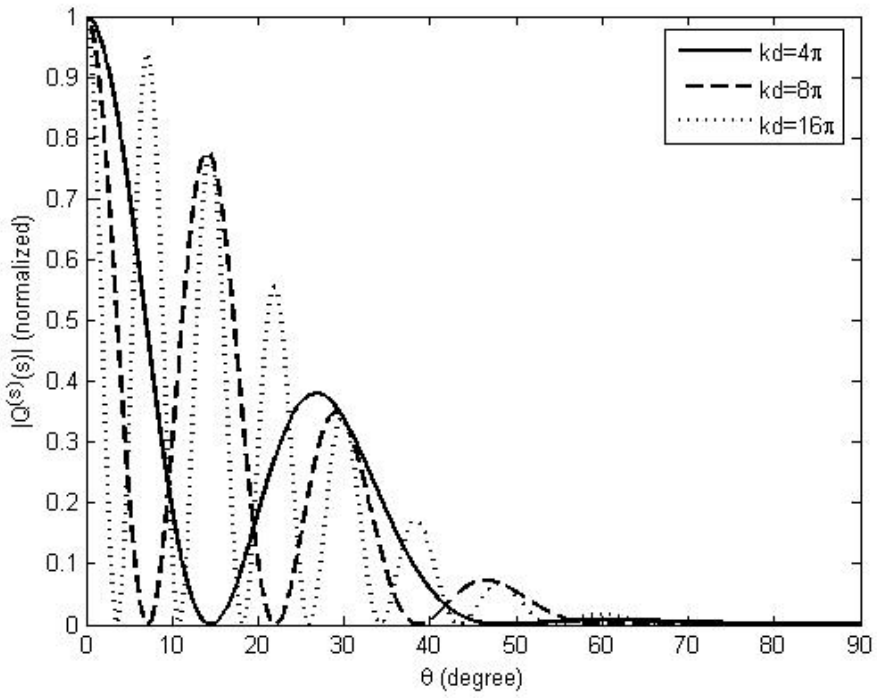

Fig. 3 (Normalized) distribution of momentum flow of the far field scattered from a pair of symmetrically distributed particles (Fig. 2(a)) for various seperation d as a function of angle θ, with $\sigma = 0.3\lambda$.

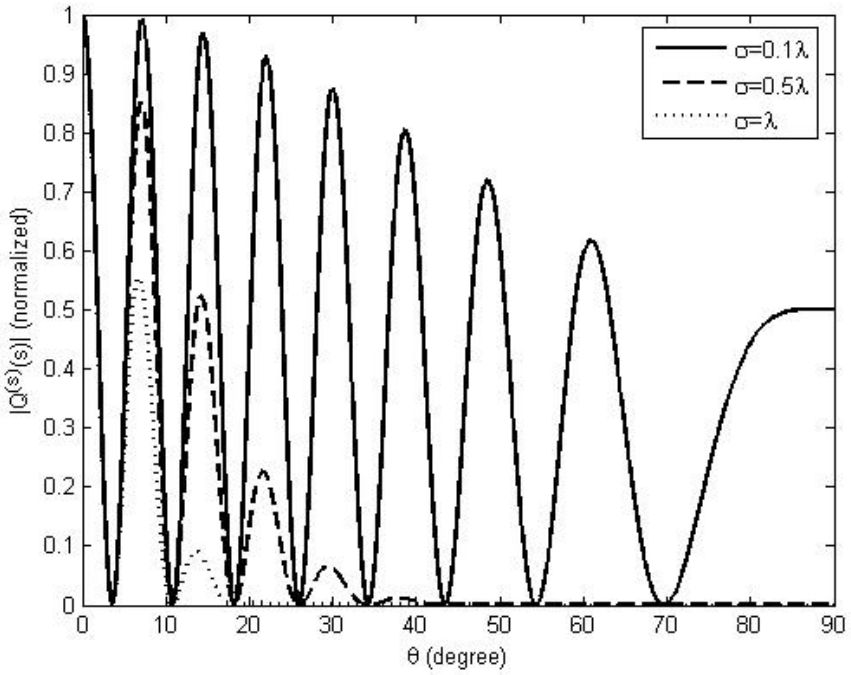

Fig. 4 (Normalized) distribution of momentum flow of the far field scattered from a pair of symmetrically distributed particles (Fig. 2(a)) for various particel size σ as a function of angle θ, with $kd = 16\pi$.

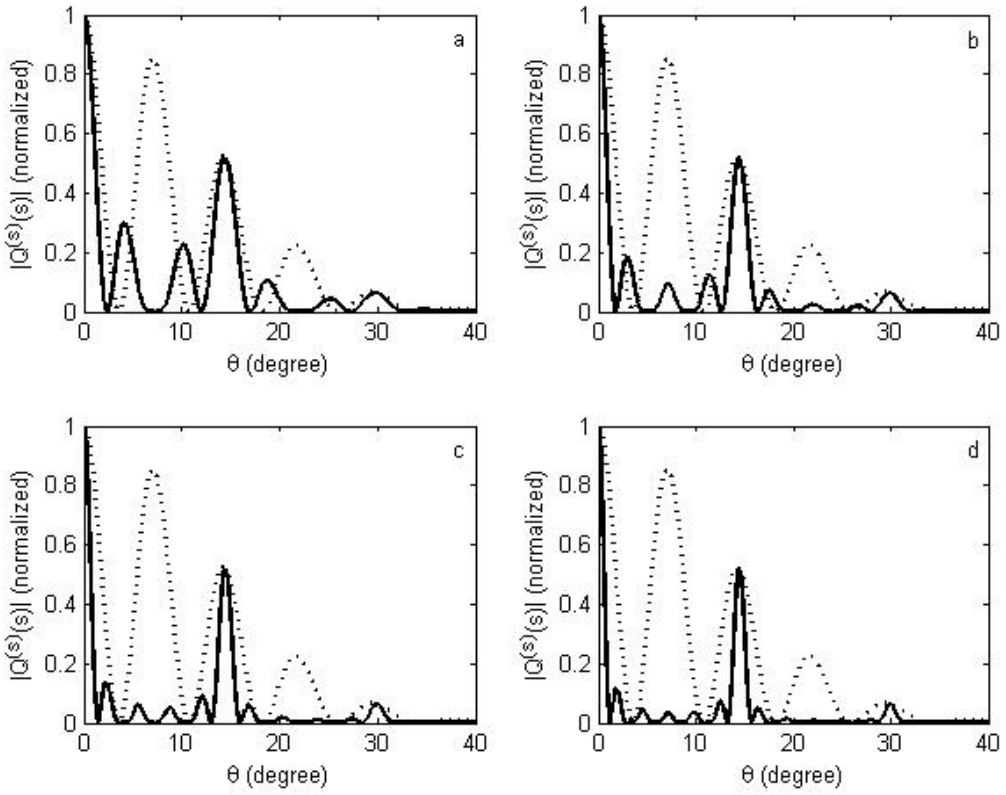

Fig. 5 (Normalized) distribution of momentum flow of the far field scattered from collections of particles shown in Fig. 2(a) (dotted curve) and (a) in Fig. 2(b) (solid curve); (b) in Fig. 2(c) (solid curve); (c) in Fig. 2(d) (solid curve); (d) in Fig. 2(e) (solid curve) with $kd = 16\pi$ and $\sigma = 0.5\lambda$.

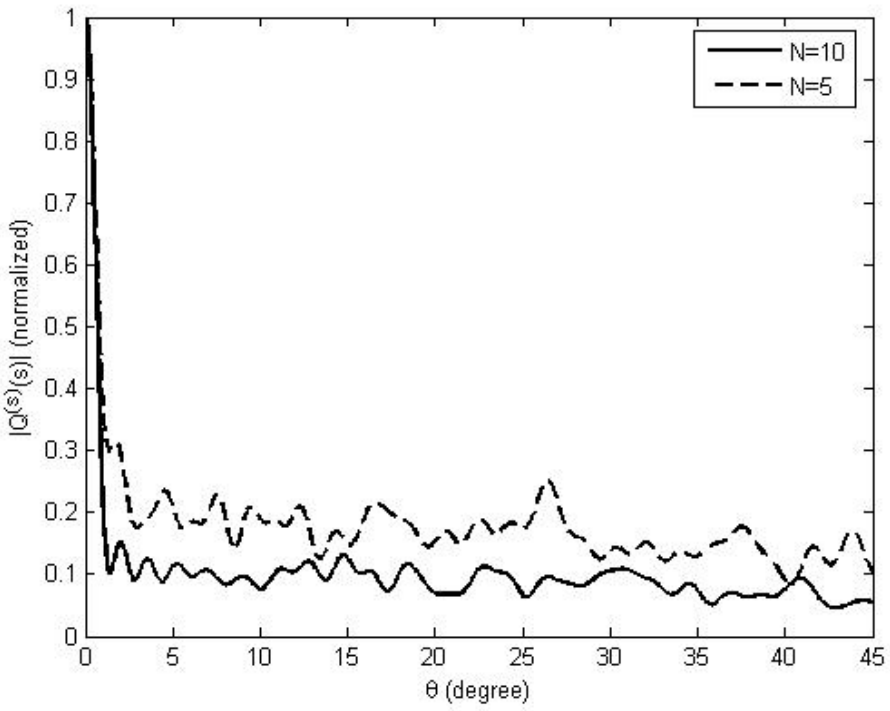

Fig. 6 (Normalized) distribution of momentum flow of the far field scattered from collections of particles randomly distributed with $\sigma = 0.1\lambda$.

Spacing distance d_{sp}	Counting numbers	Peak positions $\sin\theta$ (up to first major maximum)
$d/2$	8	$1/4$
d	7	$1/8, 1/4$
$3d/2$	6	$1/12, 1/6, 1/4$
$2d$	4	$1/16, 1/8, 3/16, 1/4$
$5d/2$	4	$1/20, 1/10, 3/20, 1/5, 1/4$
$3d$	5	$1/24, 1/12, 1/8, 1/6, 5/24, 1/4$
$7d/2$	4	$1/28, 1/14, 3/28, 1/7, 5/28, 3/14, 1/4$
$4d$	3	$1/32, 1/16, 3/32, 1/8, 5/32, 3/16, 7/32, 1/4$
$9d/2$	2	$1/36, 1/18, 1/12, 1/9, 5/36, 3/18, 7/36, 2/9, 1/4$
$5d$	1	$1/40, 1/20, 3/40, 1/10, 1/8, 3/20, 7/40, 1/5, 9/40, 1/4$

Table 1 List of all the possible spacing distances with counting numbers and peak positions for the set-up in Fig. 2(e).